A Solid Acid Catalyst at the Threshold of Superacid Strength: NMR, Calorimetry, and Density Functional Theory Studies of Silica-Supported Aluminum Chloride

Teng Xu,[†] Nick Kob,[‡] Russell S. Drago,*[,‡] John B. Nicholas,*[,§] and James F. Haw*[,†]

Contribution from the Laboratory for Magnetic Resonance and Molecular Science, Department of Chemistry, Texas A&M University College Station, Texas 77843, Catalysis Center, Department of Chemistry, University of Florida, Gainesville, Florida 32611, and Environmental Molecular Sciences Laboratory, Pacific Northwest National Laboratory, Richland, Washington 99352

Received March 17, 1997. Revised Manuscript Received July 23, 1997[⊗]

Abstract: Solid state NMR, calorimetry, and density functional theory (DFT) all provide a consistent interpretation of the acidity of the solid acid catalyst $(SG)_nAlCl_2$, which is prepared by reacting aluminum chloride with conditioned silica gel. These studies firmly establish that the acid sites are Brønsted in nature and that their strength is significantly greater than those in zeolites. Proton NMR results, including experiments exploiting $^1H-^{27}Al$ dipolar couplings, demonstrate that the Brønsted acid sites have an isotropic ^1H chemical shift of 5.7 ppm and a concentration of 0.58 mmol/g. The strongest sites on this solid acid, present at 0.03 mmol/g, have $-\Delta H_{av}$ values of 52 kcal/mol for reaction with pyridine. A value of 44 kcal/mol is maintained for incremental addition of pyridine up to 0.1 mmol/g. In comparison, $-\Delta H_{av}$ for the strongest sites in zeolite HZSM-5 is only 42 kcal/mol. ^{15}N magic angle spinning (MAS) NMR studies of adsorbed pyridine and ^{31}P MAS NMR of trimethylphosphine confirm the Brønsted nature of these acid sites. The ^{13}C isotropic chemical shift of acetone-*2*-^{13}C on $(SG)_nAlCl_2$ (245 ppm) is identical to that measured in 100% H_2SO_4. ^{13}C in situ NMR studies of ethylene and propene oligomerization show that the activity of $(SG)_nAlCl_2$ is far greater than that of zeolites. Cyclopentenyl carbenium ions are formed in significant yields in those reactions as well as during skeletal isomerization and cracking of cyclohexane at 433 K on $(SG)_nAlCl_2$. Local DFT calculations at the SVWN/DZVP2 level were used to provide predictions of the structure and energetics of the catalyst. The acidity (defined as the deprotonation energy corrected for zero-point and thermal contributions) obtained from these calculations ranges from 275.5 to 293.4 kcal/mol. Two of the three $(SG)_nAlCl_2$ models considered are more strongly acidic than a HZSM-5 cluster model treated at the same level of theory. The aggregate evidence from this study strongly supports classification of $(SG)_nAlCl_2$ as a catalyst with a Brønsted acid strength on the threshold of superacidity.

Introduction

The strength of solid acid catalysts, and hence their mechanism of action, has been the focus of much attention.[1−3] Given the present need to replace corrosive liquid acids with environmentally safer solid acids in large-scale industrial processes,[4−6] this attention will only increase. Important to the study of solid acid catalysis is the accurate determination of acid strength. Until recently, many familiar solid acid catalysts were classified as superacids,[7] i.e., acids stronger than 100% H_2SO_4. However, spectroscopic studies of reaction intermediates and probe molecules as well as combined experimental and theoretical treatments have reclassified the strength of zeolite solid acids[8,9] as being significantly weaker than superacids. The suggested superacidity of sulfated zirconia has also been questioned.[10−13] $HBr/AlBr_3$ quantitatively protonates benzene,[14,15] easily qualifying this solid as a superacid, but unsupported metal halides generate copious amounts of solid and liquid wastes and hence are no longer acceptable for many large-scale catalytic applications.

Drago and co-workers have described a unique solid acid catalyst (referred to as $(SG)_nAlCl_2$) formed by the reaction of aluminum chloride with silica gel under carefully controlled conditions.[16−20] The silica gel must be first conditioned to form a specified range of surface silanols. The silica is then reacted with aluminum chloride in refluxing CCl_4. Improper condition-

* Authors to whom correspondence should be addressed.
[†] Texas A&M University.
[‡] University of Florida.
[§] Pacific Northwest National Laboratory.
[⊗] Abstract published in *Advance ACS Abstracts,* December 1, 1997.

(1) Corma, A. *Chem. Rev.* **1995**, *95*, 559−614.
(2) Farneth, W. E.; Gorte, R. J. *Chem. Rev.* **1995**, *95*, 615−635.
(3) van Santen, R. A.; Kramer, G. J. *Chem. Rev.* **1995**, *95*, 637−660.
(4) Armor, J. N. *Environmental Catalysis*; Armor, J. N., Ed.; American Chemical Society: Washington, DC, 1994.
(5) Cusumano, J. A. *Chemtech* **1992**, *22*, 482−489.
(6) Bell, A. T.; Manzer, L. E.; Chen, N. Y.; Weekman, V. W.; Hegedus, L. L.; Pereira, C. J. *Chem. Eng. Prog.* **1995**, *91*, 26−34.
(7) Tanabe, K.; Misono, M.; Ono, Y.; Hattori, H. *New Solid Acids and Bases Their Catalytic Properties*; Elsevier: Amsterdam, 1989; Vol. 51.
(8) Haw, J. F.; Nicholas, J. B.; Xu, T.; Beck, L. W.; Ferguson, D. B. *Acc. Chem. Res.* **1996**, *29*, 259−267.
(9) Drago, R. S.; Dias, S. C.; Torrealba, M.; de Lima, L. *J. Am. Chem. Soc.* **1997**, *119*, 4444−4452.
(10) Kustov, L. M.; Kazansky, V. B.; Figuearas, F.; Tichit, D. *J. Catal.* **1994**, *150*, 143−149.
(11) Adeeva, V.; de Haan, J. W.; Janchen, J.; Lei, G. D.; Schunemann, V.; van de Ven, L. J. M.; Sachtler, W. M. H.; van Santen, R. A. *J. Catal.* **1995**, *151*, 364−372.
(12) Farcasiu, D.; Ghenciu, A.; Li, J.-Q. *J. Catal.* **1996**, *158*, 116−127.
(13) Drago, R. S.; Kob, N. *J. Phys. Chem.* **1997**, *101*, 3360−3364.
(14) Xu, T.; Barich, D. H.; Torres, P. D.; Haw, J. F. *J. Am. Chem. Soc.* **1997**, *119*, 406−414.
(15) Farcasiu, D. *Acc. Chem. Res.* **1982**, *15*, 46−51.
(16) Drago, R. S.; Getty, E. E. U.S. Patent No. 4,719,190, 1988.
(17) Drago, R. S.; Getty, E. E. *J. Am. Chem. Soc.* **1988**, *110*, 3311−3312.
(18) Drago, R. S.; Getty, E. E. U.S. Patent No. 4,929,80, 1990.
(19) Getty, E. E.; Drago, R. S. *Inorg. Chem.* **1990**, *29*, 1186−1192.
(20) Drago, R. S.; Petrosius, S. C.; Chronister, C. W. *Inorg. Chem.* **1994**, *33*, 367−372.

S0002-7863(97)00850-0 CCC: $14.00

ing of the silica or use of protic solvents yields materials of weaker acid strength. Previous work has shown that $(SG)_nAlCl_2$ has extremely high activity for the isomerization and cracking of alkanes,[17,19,21,22] e.g., isobutane, *n*-pentane, and *n*-hexadecane. The high reactivity of $(SG)_nAlCl_2$ suggests unusually strong acidity and motivated our present attempt at providing a more quantitative assessment of the catalyst's acid strength.

The $(SG)_nAlCl_2$ catalyst has been previously characterized by the Drago group using calorimetric measurements of the enthalpy of binding of pyridine to acid sites, IR of pyridine adsorbed on the catalyst, and ^{27}Al and ^{29}Si NMR.[19,20] IR studies of a catalyst sample saturated with pyridine revealed the presence of both Brønsted acid and weaker hydrogen-bonding sites. Tetrahedral aluminum was observed on the catalyst by ^{27}Al solid state NMR. It was noted during synthesis that 1 mol of HCl was released for each mole of $AlCl_3$ reacted with the silica. From this evidence, Drago and co-workers proposed that the active site was formed by the reaction of $AlCl_3$ with a silanol to form $\equiv Si-O-AlCl_2$ and HCl. Coordinate covalent bonding of a second silanol unit to the aluminum yields an acidic bridging hydroxyl analogous to the Brønsted site in zeolites ($\equiv Si-O-AlCl_2-O(H)-Si\equiv$). Reaction of nearby silanol groups in this manner should yield cyclic structures, and **1a**,**b** were proposed by Drago as possible models of the acid site.[20] In the present investigation we also theoretically consider the homologue **1c**, which has a ring size common to aluminosilicate zeolite structures.

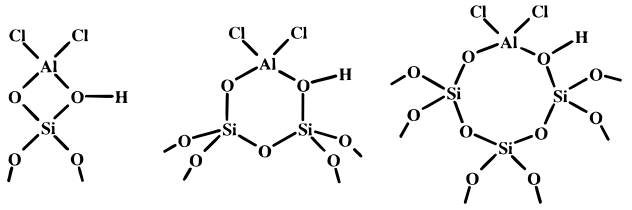

1a **1b** **1c**

The possibility of acidity greater than that of zeolites is expected from the proposed structures of $(SG)_nAlCl_2$. Whereas Al in zeolites is coordinated to four oxygens, in the proposed structures, two of the valencies of Al contain Cl. The increased electron-withdrawing ability of Cl relative to O should stabilize the conjugate base of the acid, leading to increased acidity.

Here we report detailed characterization of the acidity of $(SG)_nAlCl_2$ using NMR and theoretical methods very similar to those applied to characterize zeolite acidity.[8] These results, as well as new calorimetric studies of reactions with pyridine and 2,6-lutidine, highlight the unique properties of $(SG)_nAlCl_2$ and demonstrate that this catalyst has a strength on the threshold of superacidity.

Experimental Section

Reagents. $AlCl_3$ (99.99%) and trimethylphosphine (97%) were purchased from Aldrich. Acetone-*2*-^{13}C and pyridine-^{15}N were obtained from Isotec. Ethylene-$^{13}C_2$, propene-*2*-^{13}C, and cyclohexane-$^{13}C_1$ were purchased from Cambridge Isotope. *trans*-Stilbene-$^{13}C_2$ was obtained from C/D/N.

Catalyst Preparation. Davison silica gel 80−200 mesh was preconditioned as follows. The silica was washed with 1 M HCl, followed by deionized water, 30% H_2O_2, and then again deionized water. The peroxide treatment enhances the hydroxyl concentration compared to that of the material described in previous reports and leads to a slight increase in the strong acidity of the final catalyst. After being washed, the silica was dried at 373 K overnight in vacuum. It is critical to remove excess water without dehydrating the silanol groups. When aluminum chloride reacts with silanols on the silica surface, Al_2Cl_6 is cleaved and HCl is released. If the catalyst support is too dry, the lack of silanols causes dimeric chloro-bridged aluminum species to form on the surface. One can monitor proper preconditioning of the silica gel with TGA. Unconditioned silica gel undergoes an 8% water loss and the properly conditioned material about 4% when heated under flowing nitrogen to 773 K with a 5 K/min ramp. Silica dried at temperatures above 423 K loses much less than 4% water.

One gram of preconditioned silica as described above was refluxed in dry CCl_4 for 2 h. Anhydrous aluminum chloride (0.5 g) was then added to the stirring mixture. This mixture was allowed to react for 2 days, during which the color of the solution changed to dark purple. The mixture was then filtered in a drybox; the catalyst is very moisture sensitive, and any contact with moisture must be avoided, otherwise activity is lost.

Surface area BET analysis for the silica support and $(SG)_nAlCl_2$ catalyst are shown in Table 1. Upon preparation the surface area and pore volume of the $(SG)_nAlCl_2$ catalyst were reduced, e.g., the surface area decreased from 265 to 215 m^2/g, consistent with grafting of aluminum chloride onto the surface. The chlorine and aluminum contents of the active catalyst were carefully determined using neutron activation analysis. Samples were sealed in a glovebox prior to transfer to the reactor. This procedure eliminated the possibility of reaction with water or other changes in composition that might occur during the analysis of this material by routine methods. Duplicate analysis gave the following weight percents: chlorine 17.7% and 19.5%, mean of 18.6%; aluminum 7.2% and 7.4%, mean of 7.3%. These results are in quantitative agreement with values expected on the basis of complete reaction of aluminum chloride with silica gel and evolution of 1 mol of HCl. Since these numbers imply 2.7 mmol of Al/g of catalyst, and the concentration of Brønsted sites, reported below, is only 0.6 mmol/g, aluminum oxychloride species that are Lewis but not Brønsted sites must also form (as is observed). The nature of these species and their relation to the hydroxyl functionality of the silica were reported earlier along with a more detailed discussion of the stoichiometry of the reaction.[19]

Table 1. BET Analysis for Davison Silica Gel and $(SG)_nAlCl_2$

catalyst/support	surface area (m^2/g)	pore volume (cm^3/g)	av pore size (Å)
Davison silica	265	1.1	175
$(SG)_nAlCl_2$	215	0.76	140

Calorimetric Measurements. Acidity measurements by calorimetry[23,24] were carried out using 1 g of catalyst slurried in cyclohexane (dried over P_2O_5 and distilled) with pyridine solution. Injections of known quantities of pyridine were made to the stirred catalyst in cyclohexane, and the heat evolved from the reaction was measured after each injection. The calorimeter is equipped with a thermistor which is calibrated prior to each run. The measured heat evolved is then converted to an average enthalpy of sites titrated by determining the amount of pyridine on the solid. The complete calorimetry−adsorption (cal−ad) analysis[23] was not carried out in this investigation because pyridinium chloride forms, complicating the spectral determination of the free pyridine in solution. Therefore, the enthalpies reported are lower limits; the site amounts are approximate (±0.02 mmol/g), and equilibrium constants were not determined.

Sample Preparation for MAS NMR. To ensure a homogeneous distribution of adsorbates on the catalyst, shallow bed CAVERN devices[25,26] were used throughout this investigation to prepare samples for MAS NMR. Typically, 0.4 g (7.5-mm rotor) or 0.1 g (5-mm rotor) of $(SG)_nAlCl_2$ was loaded into a shallow-bed CAVERN under N_2

(21) Drago, R. S.; Petrosius, S. C.; Kaufman, P. B. *J. Mol. Catal.* **1994**, *89*, 317−328.
(22) Drago, R. S.; Petrosius, S. C.; Kaufman, P. B. *New J. Chem.* **1994**, *18*, 937−939.
(23) Lim, Y. Y.; Drago, R. S.; Babich, M. W.; Wong, N.; Doan, P. E. *J. Am. Chem. Soc.* **1987**, *109*, 169−174.
(24) Chronister, C. W.; Drago, R. S. *J. Am. Chem. Soc.* **1993**, *115*, 4793−4798.
(25) Munson, E. J.; Murray, D. K.; Haw, J. F. *J. Catal.* **1993**, *141*, 733−736.
(26) Xu, T.; Haw, J. F. *Topics Catal.* **1997**, *4*, 109−118.

atmosphere inside a drybox and evacuated to a final pressure of less than 10^{-4} Torr. All adsorptions were done at ambient temperature except for ethylene and propene, which were done at 77 K. The catalyst was loaded into the rotor within the CAVERN following adsorptions, and the rotor was then capped and transferred to the NMR probe.

NMR Spectroscopy. Solid state NMR experiments were performed with magic angle spinning on a modified Chemagnetics CMX-300 MHz spectrometer operating at 299.6 MHz for ^{1}H, 75.4 MHz for ^{13}C, 30.4 MHz for ^{15}N, 78.1 MHz for ^{27}Al, and 121.3 MHz for ^{31}P. Acetone (2.11 ppm), hexamethylbenzene (17.4 ppm), [^{15}N]glycine (−347.6 ppm), 0.1 M $Al(H_2O)_6^{3+}$ (0.0 ppm), tetramethylsilane (0.0 ppm), and 85% H_3PO_4 (0.0 ppm) were used as external chemical shift standards for ^{1}H, ^{13}C, ^{15}N, ^{27}Al, and ^{31}P, respectively. ^{1}H, ^{13}C, and ^{29}Si chemical shifts are reported relative to TMS, ^{15}N chemical shifts relative to nitromethane, ^{27}Al chemical shifts relative to 0.1 M $Al(H_2O)_6^{3+}$, and ^{31}P chemical shifts relative to 85% H_3PO_4. Chemagnetics-style pencil probes spun 7.5-mm zirconia rotors at 4−6.5 kHz and 5-mm zirconia rotors at 10−13 kHz with active spin speed control (±3 Hz).

Theoretical Methods

Three possible models for the catalyst active site were studied. These were derived from **1a**−**c** by satisfying unfilled valencies by suitable terminal groups. In each case the structures were fully optimized using modern analytical gradient techniques.[27,28] Cartesian coordinates are published as Supporting Information. To assess the acidity of the proposed models, the deprotonated (anionic) analogues were also fully optimized. The difference in total energy between the neutral and deprotonated models, corrected for zero-point energy (ZPE) and vibrational effects, gives a measure of the relative acid strength. All calculations were done using local density functional theory (DFT)[29−31] with the Slater[32] exchange functional and the Vosko−Wilk−Nossair[33] correlation functional (SVWN). Calculations at the local DFT level have been shown to generally give reasonable geometries and energetics.[34−38] The double-ζ polarized (DZVP2) basis sets of Godbout and co-workers[39] were used in all cases. These basis sets were optimized for use with DFT and have been shown to give better results than conventional Hartree−Fock basis sets in DFT calculations.[40] Frequency calculations (298.15 K and 1 atm) were used to verify that optimized geometries were stable points on the potential energy surface and also to obtain the ZPE and vibrational energy contributions. All calculations were done using the program Gaussian94.[41]

Results

^{27}Al and ^{1}H MAS NMR. Figure 1 shows an ^{27}Al MAS spectrum of $(SG)_nAlCl_2$ obtained at 7.05 T; the spectral lines measured at this field strength reflect both chemical shift and quadrupole effects and are similar to previously published results.[19,20] The line with a peak maximum near 70 ppm reflects the tetrahedral aluminum centers that are responsible for the Brønsted acidity of $(SG)_nAlCl_2$ as depicted in model structures **1a**−**c**. The peak at −2 ppm is indicative of a small amount of octahedral aluminum, which presumably forms due to exposure to moisture during preparation or handling steps. Although consistent with the initial reports,[20] these results differ from those reported by another group.[42] In the latter case, the spectra suggest that the sample was overdried, leading to a sample with excess aluminum chloride.

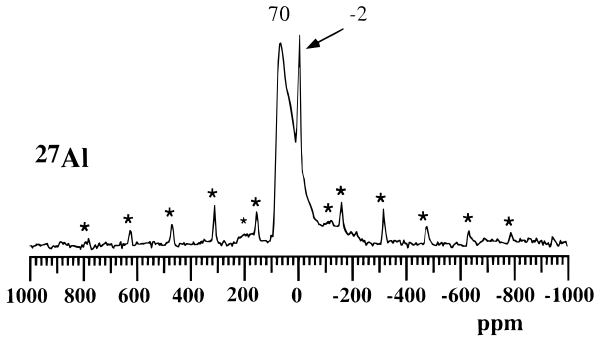

Figure 1. 78.1-MHz ^{27}Al MAS spectrum of $(SG)_nAlCl_2$. The spectrum was acquired in a 5-mm rotor with a flip angle of less than 10° (0.5-μs pulse width) and a spinning speed of 12 200 Hz and was the average of 10 000 scans with a 0.1-s pulse delay. The asterisks indicate the spinning sidebands.

^{1}H MAS spectra of the catalyst (cf. Figure 2a) showed two isotropic chemical shifts: one at 2.5 ppm due to unreacted silanol groups and the second at 5.7 ppm, which we will show to be due to the Brønsted sites (see below). Proton spin count experiments were performed to quantify the Brønsted sites. We acquired ^{1}H spectra of standards such as hexamethylbenzene and adamantane under the same spectrometer conditions as those used for acquiring ^{1}H spectra of $(SG)_nAlCl_2$. The amount of standard was adjusted so that the integrated intensity of the standard was close to that of the 5.7 ppm resonance, and the site concentration was then determined by comparison of integrations and weights. We determined that the samples of $(SG)_nAlCl_2$ used in this investigation had 0.58 mmol/g of sites represented by the 5.7 ppm resonance in the ^{1}H MAS spectrum.

Unambiguous assignment of this 5.7 ppm resonance to a hydroxyl site associated with aluminum was made using the ^{1}H−^{27}Al spin−echo experiment reported by Beck and applied to ^{1}H assignments in zeolites.[43,44] This method cleanly edited the proton spectrum of $(SG)_nAlCl_2$ into signals due to protons spatially remote from (Figure 2b) and close to (Figure 2c) aluminum.

Probe Molecule Studies. The acidity of $(SG)_nAlCl_2$ was probed with ^{15}N NMR and calorimetric studies of pyridine

(27) Johnson, B. G.; Frisch, M. J. *J. Chem. Phys.* **1994**, *100*, 7429−7442.
(28) Johnson, B. G.; Frisch, M. J. *Chem. Phys. Lett.* **1993**, *216*, 133−140.
(29) Andzelm, J. In *Density Functional Methods in Chemistry*; Labanowski, J., Andzelm, J., Eds.; Springer-Verlag: New York, 1991; p 155.
(30) Parr, R. G.; Yang, W. *Density-Functional Theory of Atoms and Molecules*; Oxford University: New York, 1989.
(31) Labanowski, J.; Andzelm, J. *Density Functional Methods in Chemistry*; Labanowski, J., Andzelm, J., Eds.; Springer-Verlag: New York, 1991.
(32) Slater, J. C. *Phys. Rev.* **1937**, *51*, 846−851.
(33) Vosko, S. J.; Wilk, L.; Nussair, M. *Can. J. Phys.* **1980**, *58*, 1200−1211.
(34) Johnson, B. G.; Gill, P. M.; Pople, J. A. *J. Chem. Phys.* **1993**, *98*, 5612−5626.
(35) Stave, M. S.; Nicholas, J. B. *J. Phys. Chem.* **1993**, *97*, 9630−9641.
(36) Stave, M. S.; Nicholas, J. B. *J. Phys. Chem.* **1995**, *99*, 15046−15061.
(37) Ziegler, T. *Chem. Rev.* **1991**, *91*, 651−667.
(38) Jones, R. O.; Gunnarsson, O. *Rev. Mod. Phys.* **1989**, *61*, 689−746.
(39) Godbout, N.; Salahub, D. R.; Andzelm, J.; Wimmer, E. *Can. J. Chem.* **1992**, *70*, 560−571.
(40) Dixon, D. A. In *Density Functional Methods in Chemistry*; Labanowski, J., Andzelm, J., Eds.; Springer-Verlag: New York, 1991.
(41) Frisch, M. J.; Trucks, G. W.; Schlegal, H. B.; Gill, P. M. W.; Johnson, B. G.; Robb, M. A.; Cheeseman, J. R.; T. Keith; Petersson, G. A.; Montgomery, J. A.; Raghavachari, K.; Al-Laham, M. A.; Zakrzewski, V. G.; Ortiz, J. V.; Foresman, J. B.; Cioslowski, J.; Stefanov, B. B.; Nanayakkara, A.; Challacombe, M.; Peng, C. Y.; Ayala, P. Y.; Chen, W.; Wong, M. W.; Andres, J. L.; Replogle, E. S.; Gomperts, R.; Martin, R. L.; Fox, D. J.; Binkley, J. S.; Defrees, D. J.; Baker, J.; Stewart, J. P.; Head-Gordon, M.; Gonzalez, C.; Pople, J. A. *Gaussian 94, Revision B.2.*; Frisch, M. J., Trucks, G. W., Schlegal, H. B., Gill, P. M. W., Johnson, B. G., Robb, M. A., Cheeseman, J. R., Keith, T., Petersson, G. A., Montgomery, J. A., Raghavachari, K., Al-Laham, M. A., Zakrzewski, V. G., Ortiz, J. V., Foresman, J. B., Cioslowski, J., Stefanov, B. B., Nanayakkara, A., Challacombe, M., Peng, C. Y., Ayala, P. Y., Chen, W., Wong, M. W., Andres, J. L., Replogle, E. S., Gomperts, R., Martin, R. L., Fox, D. J., Binkley, J. S., Defrees, D. J., Baker, J., Stewart, J. P., Head-Gordon, M., Gonzalez, C., Pople, J. A., Eds.; Gaussian, Inc.: Pittsburgh, PA, 1995.
(42) Sato, S.; Maciel, G. E. *J. Mol. Catal. A* **1995**, *101*, 153−161.
(43) Beck, L. W.; White, J. L.; Haw, J. F. *J. Am. Chem. Soc.* **1994**, *116*, 9657−9661.
(44) Beck, L. W.; Haw, J. F. *J. Phys. Chem.* **1995**, *99*, 1076−1079.

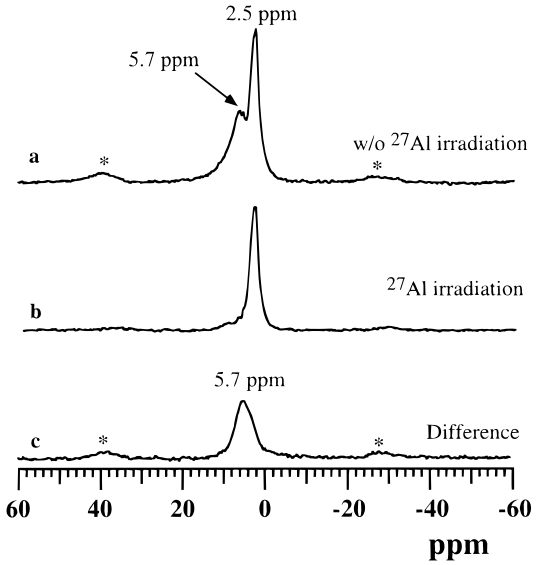

Figure 2. 299.6-MHz $^1H\{^{27}Al\}$ MAS spin−echo double-resonance experiments on $(SG)_nAlCl_2$, permitting the editing of signals due to protons dipolar coupled to aluminum. Spectra a and b were acquired at 298 K with 8-s pulse delay and 200 scans: (a) without ^{27}Al irradiation; (b) with ^{27}Al irradiation; (c) difference spectrum. The ^{27}Al irradiation field during the τ period was ca. 50 KHz. The rotor period (τ, the inverse of the spinning speed) was 100 μs. The difference spectrum selectively shows the ^1H signal of the Brønsted sites at 5.7 ppm.

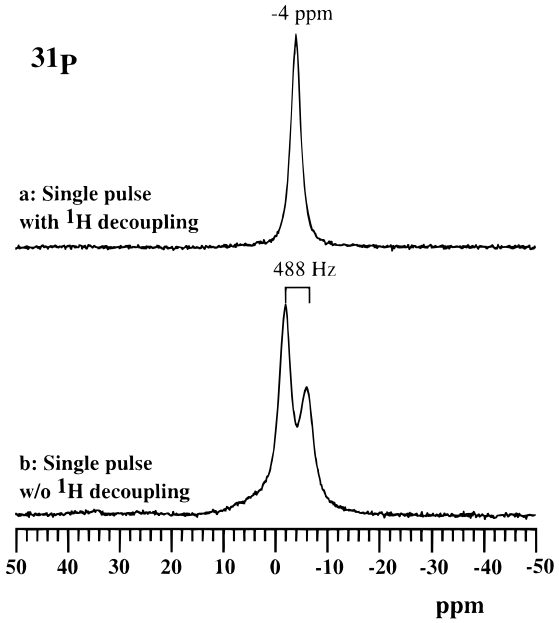

Figure 3. 120.3-MHz ^{31}P spectrum of trimethylphosphine (0.6 mmol/g) on $(SG)_nAlCl_2$. The acid sites are unambiguously shown to be Brønsted in nature. Both spectra were acquired with 40-s pulse delay and the average of 2000 scans. The proton decoupled spectrum a shows a single peak at −4 ppm, corresponding to protonated trimethylphosphine. The proton coupled spectrum b shows $^1H-^{31}P$ scalar coupling ($^1J_{^1H-^{31}P} = 488$ Hz).

adsorption as well as ^{13}C NMR studies of acetone and ^{31}P NMR of trimethylphosphine.[45,46] Figure 3 reports ^{31}P MAS spectra of 0.6 mmol/g trimethylphosphine on this catalyst; the observation of a single resonance at −4 ppm and scalar coupling,

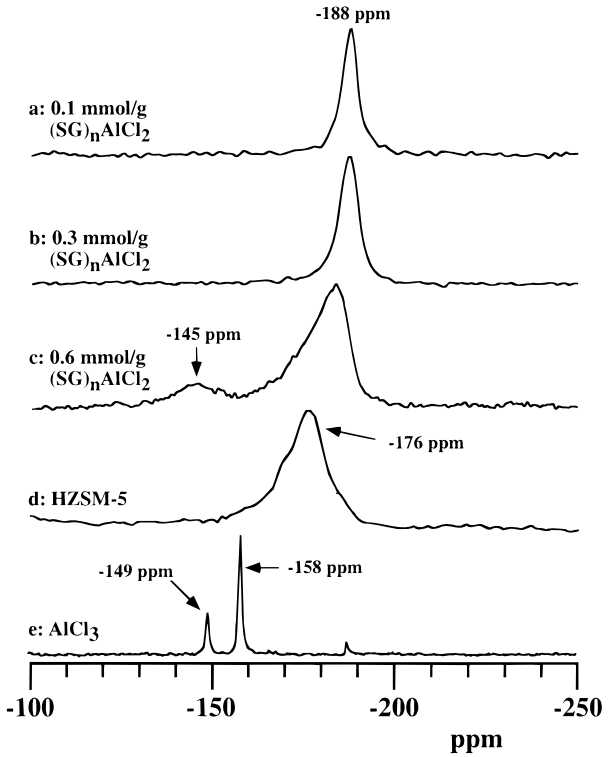

Figure 4. 30.4-MHz ^{15}N spectra of pyridine-^{15}N on $(SG)_nAlCl_2$ and other solid acids demonstrating the use of pyridine to distinguish Brønsted sites from Lewis sites. All the spectra were acquired at 298 K using cross polarization with 1 ms contact time and 1-s pulse delay except for d, where the Bloch decay pulse sequence with a 10-s pulse delay was used. The number of scans was as follows: (a) 40 000; (b) 2000; (c) 2000; (d) 40 000; (e) 200.

$^1J_{^1H-^{31}P} = 488$ Hz, is unambiguous evidence for Brønsted acid sites at the concentration expected from the ^1H spin counting experiment.

Figure 4 reports ^{15}N MAS NMR spectra of pyridine[47,48] at various loadings on $(SG)_nAlCl_2$ as well as on zeolite HZSM-5 and aluminum chloride powder. The ^{15}N isotropic shift has distinctive ranges for Brønsted and metal-centered Lewis acid sites. Pyridine-^{15}N loadings on $(SG)_nAlCl_2$ at and below 0.3 mmol/g gave a single peak at −188 ppm; this is upfield of the −176 ppm seen in zeolite HZSM-5, suggesting stronger Brønsted acidity for $(SG)_nAlCl_2$. When the pyridine loading was 0.6 mmol/g, titration of the Brønsted sites was complete, and a small peak at −145 ppm was observed and assigned to metal-centered Lewis sites associated with other aluminum oxychloride species. Pyridine on aluminum chloride powder gave signals at −158 and −149 ppm (Figure 4e). We have not made a molecular-level assignment of these peaks, but complexation with two different $(AlCl_3)_n$ species seems plausible.

The reaction of pyridine with this new preparation of $(SG)_nAlCl_2$ was studied calorimetrically. Figure 5 shows plots of $-\Delta H_{av}$ (kcal/mol) against the amount of pyridine (mmol) added in titrating acid sites. The diagram shows that enthalpies become less negative with increasing concentrations of probe molecules, indicating a reduction in strength of acid sites as the amount of titrant increases. The strongest acid sites on $(SG)_nAlCl_2$ have $-\Delta H_{av}$ of 52 kcal/mol, and a value of 44 kcal/mol is maintained up to a loading of 0.1 mmol/g. Table 2

(45) Lunsford, J. H.; Rothwell, W. P.; Shen, W. *J. Am. Chem. Soc.* **1985**, *107*, 1540−1547.
(46) Chu, P.-J.; Mallmann, A. d.; Lunsford, J. H. *J. Phys. Chem.* **1991**, *95*, 7362−7368.
(47) Maciel, G. E.; Haw, J. F.; Chuang, I.-S.; Hawkins, B. L.; Early, T. E.; McKay, D. R.; Petrakis, L. *J. Am. Chem. Soc.* **1983**, *105*, 5529−5535.
(48) Haw, J. F.; Chuang, I.-S.; Hawkins, B. L.; Maciel, G. E. *J. Am. Chem. Soc.* **1983**, *105*, 7206−7207.

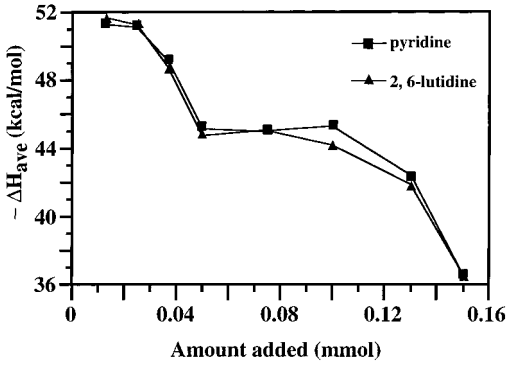

Figure 5. Diagram of $-\Delta H_{av}$ vs the amount of pyridine or 2,6-lutidine added in the calorimetric titration of acid sites showing enthalpies of binding of probe molecules to acid sites of $(SG)_nAlCl_2$. The identical behavior for the two probes is further evidence of Brønsted acidity.

Table 2. ΔH_{av} Values for Various Solid Acids from Calorimetric Titration with Pyridine

catalyst	$-\Delta H_{av}$ (kcal/mol)	ref
$(SG)_nAlCl_2$	52	this study
HZSM-5	42	9
ZrO_2-SO_4	31	13
$ZrO_2-SO_4-Fe-Mn$	26	13
SiO_2	13	24

compares $-\Delta H_{av}$ values for different solid acids; note in particular that for zeolite HZSM-5 the value is only 42 kcal/mol. Figure 5 also shows that essentially identical behavior was seen when the calorimetric experiment on $(SG)_nAlCl_2$ was repeated with 2,6-lutidine (2,6-dimethylpyridine) as the probe. This sterically hindered base complexes weakly, if at all, with metal-centered Lewis sites. The results in Figure 5 further demonstrate that the strong acidity in $(SG)_nAlCl_2$ is Brønsted in nature. The titration shows that ^{31}P and ^{15}N NMR studies of trimethylphosphine and pyridine do not discriminate 51, 45, and 36 kcal/mol Brønsted sites.

The spectroscopy and reaction chemistry of acetone on solid acids have been thoroughly examined. The isotropic shift of acetone-*2*-^{13}C changes upon complexation with either Brønsted[49−51] or Lewis acids.[52] Unfortunately the ranges of these shifts overlap, but the Brønsted nature of this catalyst is unambiguously demonstrated by the calorimetry and trimethylphosphine results. Figure 6 reports ^{13}C MAS spectra of various loadings of acetone-*2*-^{13}C on $(SG)_nAlCl_2$. Loadings at or below 0.1 mmol/g produced a single resonance at 245 ppm. At 0.5 mmol/g, resolved peaks at 245 and 242 ppm were observed at 298 K, and these reversibly coalesced at 473 K.

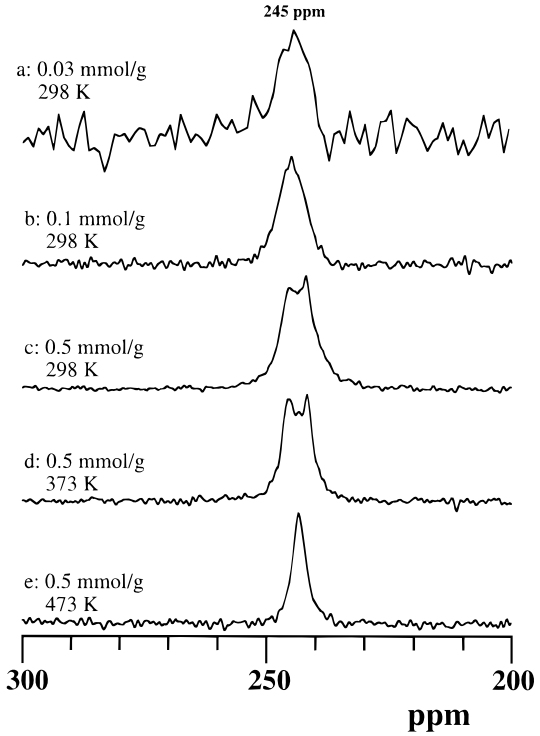

Figure 6. 75.4-MHz ^{13}C MAS spectra of acetone-*2*-^{13}C on $(SG)_nAlCl_2$ showing acidity shifts at acetone loadings of 0.03, 0.1, and 0.5 mmol/g. For clarity, only the signals in the carbonyl region are shown. Spectra a and b were acquired using cross polarization with 1-s pulse delay and 2-ms contact time, and spectra c, d, and e are Bloch decay spectra with 4-s pulse delay: (a) 180 000 scans; (b) 20 000 scans; (b, c, and d) 200 scans.

Table 3. ^{13}C Chemical Shifts of Acetone-*2*-^{13}C on a Variety of Solid and Liquid Acid Media

media	δ_{iso} (ppm)	ref
$CDCl_3$	205	53
HY	218	49
HZSM-5	223	49
100% H_2SO_4	245	54
$(SG)_nAlCl_2$	245	this study
magic acid (FSO_3H/SbF_5)	249	55, 56

Table 3 reports the ^{13}C isotropic shifts of acetone on various solid and liquid acids. The 245 peak seen here for $(SG)_nAlCl_2$ is far downfield of 223 ppm on HZSM-5. This value is identical to that observed for 100% H_2SO_4.

In Situ ^{13}C Studies of Hydrocarbon Reactions. Ethylene-$^{13}C_2$ and propene-*2*-^{13}C were adsorbed on $(SG)_nAlCl_2$ at 77 K in separate experiments, and ^{13}C MAS spectra were acquired as the temperature was raised to 298 K. Previous experiments on acidic zeolites have shown that ethylene oligomerization does not initiate until slightly above 298 K,[57] while propene begins to oligomerize at ca. 233 K.[58] As shown in Figure 7, the corresponding oligomerization reactions on $(SG)_nAlCl_2$ occurred at much lower temperatures. For propene, oligomer formation was essentially complete before the first spectrum was acquired. Figure 7 also shows the production of cyclopentenyl cations,[58,59] with substitution patterns suggested by **2** and **3**. The cyclopentenyl cations account for the signals in the vicinity of 250 and 150 ppm in Figure 7. These cations are the products of a complex series of oligomerization, rearrangement, cracking, and

(49) Xu, T.; Munson, E. J.; Haw, J. F. *J. Am. Chem. Soc.* **1994**, *116*, 1962−1972.
(50) Bosácek, V.; Kubelková, L.; Nováková, J. In *Catalysis and Adsoption by Zeolites*; Öhlmann, G., Ed.; Elsevier Science: Amsterdam, 1991.
(51) Biaglow, A. I.; Gorte, R. J.; Kokotailo, G. T.; White, D. *J. Catal.* **1994**, *148*, 779−786.
(52) Xu, T.; Torres, P. D.; Beck, L. W.; Haw, J. F. *J. Am. Chem. Soc.* **1995**, *117*, 8027−8028.
(53) Breitmeier, E.; Haas, G.; Voelter, W. *Atlas of Carbon-13 NMR Data*; Heyden & Son Ltd.: London, 1979.
(54) McClelland, R. A.; Reynolds, W. F. *Can. J. Chem.* **1976**, *54*, 718−725.
(55) Olah, G. A.; White, A. M. *J. Am. Chem. Soc.* **1968**, *90*, 1884−1889.
(56) Krivdin, L. B.; Zinchenko, S. V.; Kalabin, G. A.; Facelli, J. C.; Tufro, M. F.; Contreras, R. H.; Denisov, A. Y.; Gavrilyuk, O. A.; Mamatyuk, V. I. *J. Chem. Soc., Faraday Trans.* **1992**, *88*, 2459−2463.
(57) White, J. L.; Beck, L. W.; Haw, J. F. *J. Am. Chem. Soc.* **1992**, *114*, 6182−6189.
(58) Haw, J. F.; Richardson, B. R.; Oshiro, I. S.; Lazo, N. L.; Speed, J. A. *J. Am. Chem. Soc.* **1989**, *111*, 2052−2058.
(59) Xu, T.; Haw, J. F. *J. Am. Chem. Soc.* **1994**, *116*, 7753−7759.

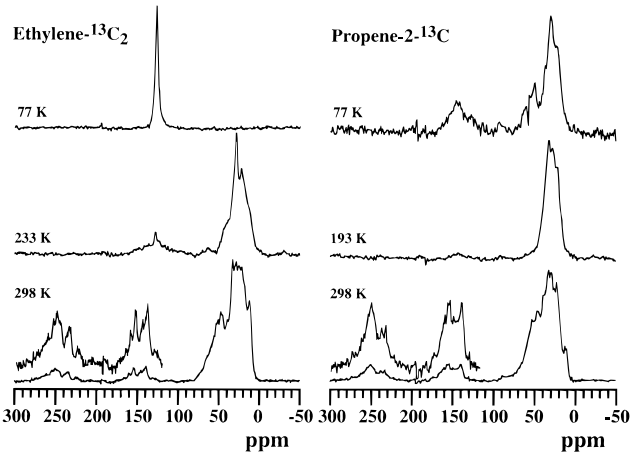

Figure 7. 75.4-MHz ^{13}C CP/MAS spectra showing in situ studies of ethylene-$^{13}C_2$ and propene-*2*-^{13}C on $(SG)_nAlCl_2$. The loadings of adsorbates are less than 0.5 mmol/g, and only cross polarization spectra are shown. Both olefins began oligomerization at low temperatures, and a considerable yield of cyclopentenyl cations was formed at 298 K as indicated by the signals in the 230−252 and 140−158 ppm regions.

Scheme 1

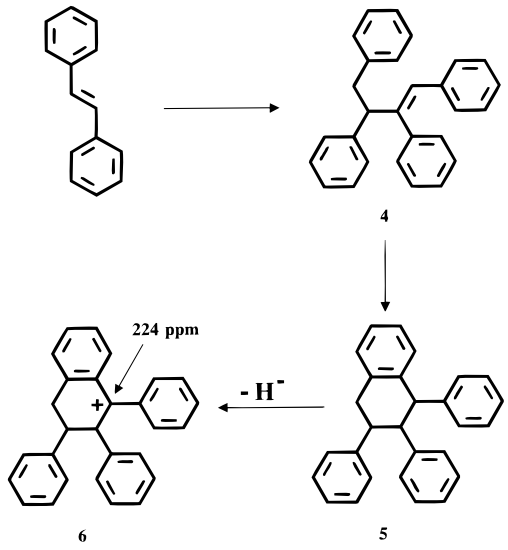

hydride transfer reactions and have been observed on zeolite solid acids[58,59] as well as aluminum chloride powder.[52]

$(SG)_nAlCl_2$ has larger pores than those found for zeolites, and we took advantage of this property to study the oligomerization of *trans*-stilbene-$^{13}C_2$ (Scheme 1). The sample was prepared by mixing 0.053 g of crystalline olefin with 0.1 g of catalyst inside a drybox, and spectra were acquired at 298 K. The spectrum first acquired (Figure 8a) suggests that ca. 50% of *trans*-stilbene (128 ppm) had dimerized to form **4** and **5**, as indicated by the 35−50 ppm signals. After 12 h at 298 K, the spectrum (Figure 8b) indicated a more extensive reaction, including the formation of carbenium ion **6** (224 ppm). This assignment is supported by a dipolar dephasing experiment[60] (cf. Figure 8c,d).

(60) Opella, S. J. *J. Am. Chem. Soc.* **1979**, *101*, 5854−5856.

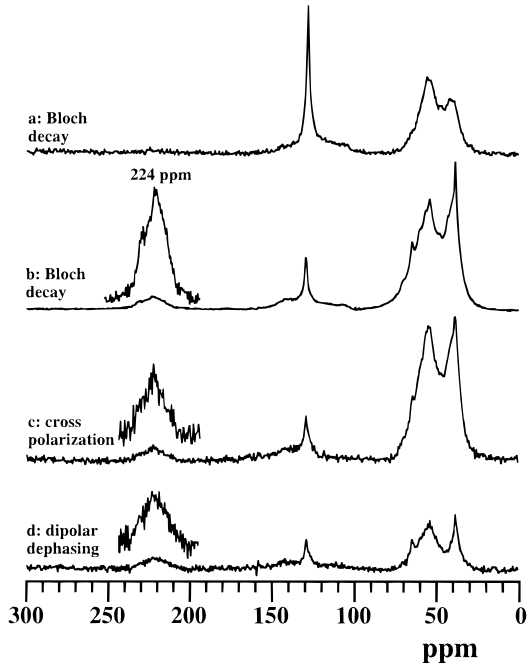

Figure 8. 75.4-MHz ^{13}C spectra of *trans*-stilbene-$^{13}C_2$ on $(SG)_nAlCl_2$ showing the formation of diphenyl carbenium ion **6**. The sample was prepared by first mixing the catalyst (0.1 g) with 0.053 g of *trans*-stilbene-$^{13}C_2$ fine powder inside a drybox. The mixture was then packed into a 5-mm NMR rotor. All of the spectra were acquired at 298 K: (a and b) Bloch decay spectrum, 40-s pulse delay; (c) cross polarization spectrum; (d) cross polarization with 50 μs of dipolar dephasing time.

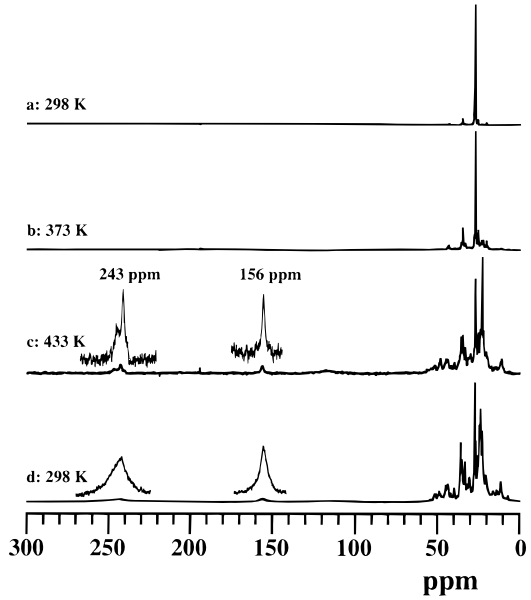

Figure 9. 75.4-MHz ^{13}C spectra of cyclohexane-$^{13}C_1$ on $(SG)_nAlCl_2$, showing skeletal isomerization and cracking reactions at moderate temperatures. The loading of cyclohexane-$^{13}C_1$ was ca. 0.6 mmol/g, and Bloch decay spectra are shown.

We also studied the skeletal isomerization of cyclohexane-$^{13}C_1$ on $(SG)_nAlCl_2$ (Figure 9). The reactant (27 ppm) formed a small amount of methylcyclopentane (35, 27, and 20 ppm) at 298 K, and cracking to isobutane (23 ppm) was important at 433 K. Again, relative to acidic zeolites,[59] this chemistry occurred at much lower temperatures on $(SG)_nAlCl_2$. Cyclopentenyl cations were observed on $(SG)_nAlCl_2$ during alkane cracking.

DFT Calculations. Three models of the catalyst active site were considered. The first of these, shown in Figure 10a, would

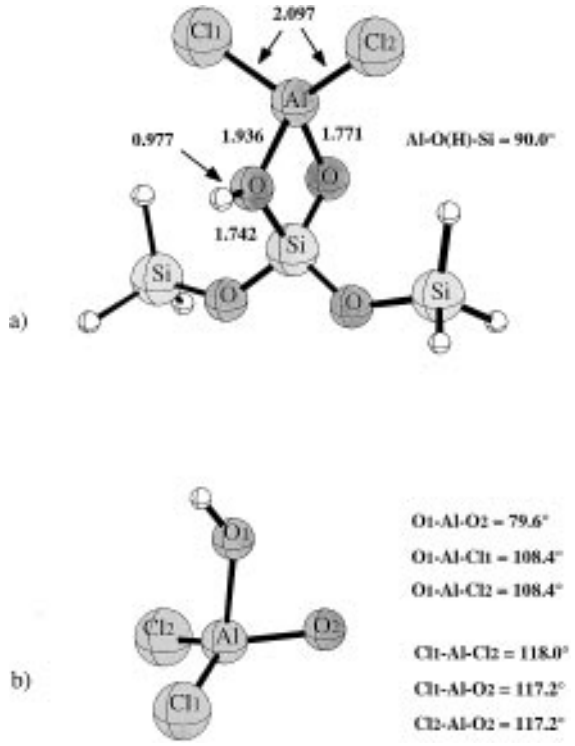

Figure 10. (a) SVWN/DZVP-optimized geometry of model **1a**. Selected bond lengths in angstroms and angles in degrees. (b) Detailed view of Al and its immediate coordination shell with distant atoms removed for clarity.

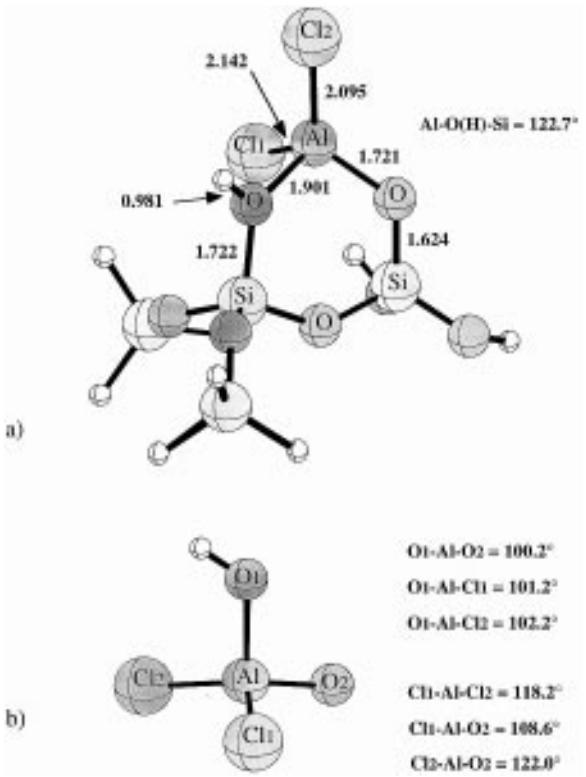

Figure 11. (a) SVWN/DZVP-optimized geometry of model **1b**. Selected bond lengths in angstroms and angles in degrees. (b) Detailed view of Al and its immediate coordination shell with distant atoms removed for clarity.

be formed by the reaction of $AlCl_3$ with a surface Si having two hydroxyls (i.e., a geminal silanol). This reaction would result in the formation of a four-membered ring. In our model, the Si in the ring is coordinated to two (H_3SiO-) groups to better simulate the silica surface. The stoichiometry of this cluster is $H_7AlSi_3O_4Cl_2$.

Several structural features of the optimized geometry are notable. First, the geometry about Al is considerably distorted from the tetrahedral configuration expected in similar materials, such as zeolites. This is better seen in Figure 10b, which provides an alternate view of the Al coordination in this model, with atoms outside of the immediate coordination sphere of Al removed for clarity. The two Cl and the unprotonated bridging oxygen are arranged in trigonal fashion about Al. The bond angles between these atoms average 117.5°, close to the value of 120° expected in an exactly trigonal environment. The Al interacts with hydroxyl oxygen through its lone pair (a dative bond). The geometry is consistent with this interpretation, as the Al−O(H) distance is considerably longer (1.936 versus 1.771 Å between Al and the unprotonated O), and the bond angles from the hydroxyl O to Al and the neighboring atoms average 98.8°. The constraint of the four-membered ring results in a H−O−Al−Cl dihedral angle of 90°. In the more flexible models considered below, this dihedral angle is close to 0°. The very small O−Al−O bond angle (79.6°) suggests that the four-membered ring is strained (see below). The appearance of strain may also be evidenced by the Al−O(H)−Si angle, which is only 90.0°. While prior calculations[61] indicate that the potential energy differences associated with changes in this bond angle can be small for angles between 180° and approximately 130°, angles as small as 90.0° are highly unfavorable. Previous calculations[61] have also shown that the acidity of the bridging hydroxyl is related to the Al−O(H)−Si angle, with smaller values of this angle associated with decreased acidity (the highest acidity would result from an angle of 180°). Consistent with these findings, the predicted acidity of this model (as defined in the section on Theoretical Methods) is 293.4 kcal/mol, considerably less acidic than the other models which allow relaxation of the Al−O(H)−Si angle (see below).

The next model considered assumes that reaction would take place between two adjacent silanol groups. The resulting six-membered ring structure is that which we initially presented as **1b** with the addition of terminal groups ($H_9AlSi_4O_7Cl_2$). The optimized geometry is shown in Figure 11a, and the closer view of Al coordination is given in Figure 11b. Similar to the four-membered ring, the geometry about Al is closer to trigonal with regard to the two Cl and unprotonated O, whereas the lone pair on the bridging hydroxyl is coordinated to the empty orbital of Al. As Figure 11b indicates, placing the Al in the larger ring allows relaxation of the geometry. The H−O−Al−Cl dihedral angle is 8.5°, indicating that Cl prefers to eclipse the acidic proton if the environment allows. In this case, the three angles associated with trigonal coordination about Al average 116.3°, and the angles associated with the bridging hydroxyl average 101.2°. The relaxation afforded by the larger ring allows Al to adopt a slightly more tetrahedral geometry. The increase on the O−Al−O angle is accompanied by decreases (≈0.04−0.05 Å) in the Al−O bond lengths compared to the four-membered ring model. There is also a large difference in the Al−O(H)−Si angle, which expands by 32.7° to 122.7° in the six-membered ring. As expected from the discussion presented above with regard to this angle, the predicted acidity of this model is notably greater, being 279.1 kcal/mol.

Although the six-membered ring model appears to be much more reasonable than placing Al in a four-membered ring, the zeolite literature gives precedence for Al in even larger rings. In this third model we place Al in an eight-membered ring. Such

(61) Nicholas, J. B.; Winans, R. E.; Harrison, R. J.; Iton, L. E.; Curtiss, L. A.; Hopfinger, A. J. *J. Phys. Chem.* **1992**, *96*, 10247−10257.

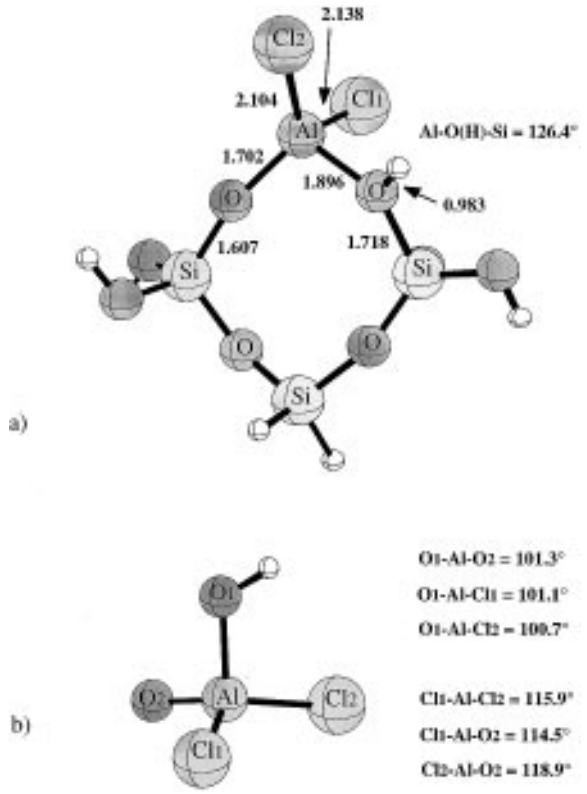

Figure 12. (a) SVWN/DZVP-optimized geometry of model **1c**. Selected bond lengths in angstroms and angles in degrees. (b) Detailed view of Al and its immediate coordination shell with distant atoms removed for clarity.

a ring would be formed by reaction with surface silanols that are separated by an additional Si−O linkage.

Figure 12a shows the optimized geometry for the eight-membered ring model ($H_7AlSi_3O_8Cl_2$). As before, Figure 12b highlights the coordination about Al. Compared to the six-membered ring, there is little change in bond lengths and angles; the largest change in a bond length is 0.019 Å for the Al−O bond. The dihedral angle formed by H−O−Al−Cl is 6.9°, similar to that in the six-membered ring. The more trigonal angles involving Al average 116.4°, while the remaining angles average 101.0°. The important Al−O(H)−Si angle expands by 3.7° compared to the value in the six-membered ring. The predicted acidity of this model is 275.5 kcal/mol, 3.6 kcal/mol more acidic than the value obtained for the six-membered ring. Consistent with the increases in acidity due to the increases in the larger Al−O(H)−Si angles with larger rings, the bond lengths between the acidic proton and the bridging oxygen also increase. Although these differences are small (0.977 Å (4-ring) to 0.981 Å (6-ring) to 0.983 (8-ring)), the trend is as expected.

The theoretical results suggest that placing Al in larger rings may allow sites of even greater acidity. However, the small difference in acidity between the six- and eight-membered ring models (3.6 kcal/mol) suggests that *significant* increases in acidity for larger rings are unlikely. Considering the apparent strain associated with the four-membered ring and the lower acidity relative to the other models, it seems that the **1a** model is less likely to account for the properties of the catalyst than either the six-membered (**1b**) or eight-membered (**1c**) ring models. It is tempting to speculate that the latter calculated acidities correspond to the 51 and 45 kcal/mol sites in the calorimetric pyridine titrations.

Although we are able to predict the acidity of our models of the $(SG)_nAlCl_2$ catalyst, these numbers by themselves do not provide a direct means by which superacidity can be determined, as there is as yet no exact experimental measurement of the deprotonation enthalpy for comparison. However, we can compare our predictions with the results of similar calculations on related solid acids. For example, we[36] and others[62] have previously studied the acidity of cluster models of the zeolite HZSM-5. The most acidic model of HZSM-5 we have previously studied is the cluster $(H_3SiO)_3-SiOHAl-(OSiH_3)_3$.[36,63] To achieve a meaningful comparison we recalculated the acidity of this model, using the same exchange-correlation functional and basis set as we used for the $(SG)_nAlCl_2$ models. In the calculations of the HZSM-5 model, the inner 10 atoms (the SiOHAl bridge and the neighboring six oxygens) were optimized while the rest of the atoms were constrained to crystal positions. Previous results indicate that further relaxation of the cluster gives values that are slightly less acidic. The predicted acidity of the HZSM-5 model at the SVWN/DZVP2 level of theory is 286.4 kcal/mol. It is of interest to note that HZSM-5 is 3 kcal/mol less acidic in the pyridine titration than the second site of $(SG)_nAlCl_2$. Consistent with our interpretation of the experimental data, we find that the six- and eight-membered ring models of $(SG)_nAlCl_2$ are notably more acidic than a strongly acidic zeolite. Although calculations with more complete basis sets, larger cluster models, and nonlocal exchange-correlation functionals might provide more definitive measures of acidity, the theoretical results are consistent with the experimental results reported here that indicate $(SG)_nAlCl_2$ is much more acidic than HZSM-5.

Discussion

The acidity of $(SG)_nAlCl_2$ is clearly Brønsted in nature. The calorimetric measurements and chemical shifts of adsorbed probe molecules consistently demonstrate that most of these sites are significantly stronger than those in zeolites. Indeed, these measurements strongly argue for a classification of $(SG)_nAlCl_2$ as a solid acid catalyst at the threshold of superacidity (strength similar to 100% H_2SO_4). $(SG)_nAlCl_2$ is not as strong an acid as magic acid or the solid acid $HBr/AlBr_3$. Both $HBr/AlBr_3$ and magic acid quantitatively protonate benzene,[14,64] whereas we did not observe benzene protonation on $(SG)_nAlCl_2$. Although superacids span a considerable range of strengths, and $(SG)_nAlCl_2$ may be strong enough to marginally qualify as a superacid, its reactivity suggests that its acid strength is well below that of magic acid, a well-established superacid. It should be emphasized, however, that in view of the different acid species involved a direct comparison of solid and solution acidity is not possible.

The strength of $(SG)_nAlCl_2$ relative to zeolites such as HZSM-5 or HY is readily apparent in calorimetry as well as in a comparison of in situ NMR studies of olefin oligomerization. We have previously used NMR to observe unreacted propene on acidic zeolites at cryogenic temperatures. Repeated attempts to see the onset of reaction of propene on $(SG)_nAlCl_2$ were unsuccessful, and the spectrum of the sample from propene at

(62) Brand, H. V.; Curtiss, L. A.; Iton, L. E. *J. Phys. Chem.* **1993**, *97*, 12773−12782.

(63) In the earlier work we used the numerical DFT program DMol. The local exchange correlation functional of von Barth and Hedin was used, although this functional should give results very close to those given by the SVWN functional used in the current study. The basis set (DNP+) used in the earlier work was also by necessity different, although it is comparable to DZVP2 in size. The most important difference is that in the earlier study only the inner three or four atoms of the acid site (≡Si−O−Al≡ or ≡Si−OH−Al≡) were allowed to optimize, whereas all other atoms were fixed in crystal positions. This limited relaxation led to an artificially greater estimate of the acidity, which is remedied in the current work.

(64) Beck, L. W.; Xu, T.; Nicholas, J. B.; Haw, J. F. *J. Am. Chem. Soc.* **1995**, *117*, 11594−11595.

77 K in Figure 7 shows oligomeric olefins. Propene characteristically forms framework-bound alkoxyl species during its oligomerization on zeolites; no analogous species were characterized on $(SG)_nAlCl_2$. These results demonstrate that the stronger acidity of $(SG)_nAlCl_2$ relative to zeolites is reflected in differences in the reactions of olefins on these catalysts.

The deprotonation energies calculated for models representing **1b**,**c** are lower than the ranges estimated for zeolitic sites at comparable levels of theory, and this is consistent with the greater acid strength for $(SG)_nAlCl_2$ relative to zeolites. All of the models considered thus far propose the reaction of a single $AlCl_3$ with silanol groups. These calculations do not in themselves rule out the possibility that more elaborate structural models would have even greater calculated acidities. Furthermore, have we not attempted to include long-range electrostatics in our calculations. Nevertheless, the theoretical results provide the first quantitative view of the structure and acidity of the proposed acid site, and the calculated acidities reported here are consistent with very strong acidities.

We have demonstrated that the solid acid catalyst $(SG)_nAlCl_2$ is a Brønsted acid with a strength intermediate between that of zeolites and magic acid. The very strong acid strength of this material is established by the extensive and varied methodologies applied here and interpreted relative to analogous studies of zeolite solid acids.

Summary

The catalyst studied in this investigation had ca. 0.58 mmol/g of Brønsted acid sites, and calorimetry showed that the strongest of these exhibited an enthalpy of reaction with pyridine that is 14 kcal/mol more exothermic than in a comparable measurement on zeolite HZSM-5. The ^1H isotropic shift of these sites is 5.7 ppm, and $^1H-^{27}Al$ experiments confirmed dipolar coupling between those protons and nearby aluminum, as required by **1a**−**c**. Calorimetry and the ^{13}C shifts of acetone show that sites are not homogeneous. The ^{13}C isotropic shift of acetone-*2*-^{13}C on the catalyst measured at coverages of below 0.1 mmol/g, 245 ppm, is identical to that measured in 100% H_2SO_4. The results of other probe molecule studies using ^{31}P NMR of trimethylphosphine and ^{15}N NMR of pyridine are also consistent with stronger Brønsted acid sites than those in zeolites. In situ ^{13}C NMR studies of the reactions of ethene and propene show olefin oligomerization at temperatures well below those required in comparable studies on acidic zeolites; the end products included large amounts of cyclopentenyl carbenium ions. Acid-catalyzed carbenium chemistry was observed for *trans*-stilbene in the mesopores of this catalyst. A ^{13}C in situ study of alkane skeletal isomerization on $(SG)_nAlCl_2$ also showed the formation of cyclopentenyl cations. Local density functional theory calculations of cluster models based on **1a**−**c** predict acidities of 293.4 kcal/mol (**1a**), 279.1 kcal/mol (**1b**), and 275.5 kcal/mol (**1c**). The latter values are ca. 7−11 kcal/mol lower than the acidity predicted for a comparable HZSM-5 zeolite model at the same level of theory, in agreement with the experimental finding of greater acid strength for $(SG)_nAlCl_2$ versus zeolite solid acids.

Acknowledgment. Work done at Texas A&M was supported by the U.S. Department of Energy (DOE) Office of Basic Energy Sciences (BES) (Grant No. DE-FG03-93ER14354). J.B.N. is supported by the U.S. DOE-BES. Computer resources were provide by the National Energy Research Supercomputer Center (NERSC), Berkeley, CA, the Texas A&M University Supercomputing Facility, and the National Center for Supercomputing Applications, Champaign, IL. Pacific Northwest National Laboratory is a multiprogram national laboratory operated by Battelle Memorial Institute for the DOE.

Supporting Information Available: Tables describing catalyst models (4 pages). See any current masthead page for ordering and Internet access instructions.

JA970850N